https://doi.org/10.17221/10/2022-RAE

Dielectric properties of materials for 3D printing at high frequencies

Tomáš Pícha[1,2], Stanislava Papežová[1]*

[1]*Department of Electrical Engineering and Automation, Faculty of Engineering, Czech University of Life Sciences Prague, Prague, Czech Republic*
[2]*Department of Agricultural Machines, Faculty of Engineering, Czech University of Life Sciences Prague, Prague, Czech Republic*

**Corresponding author: pichat@tf.czu.cz*

Citation: Pícha T., Papežová S. (2023): Dielectric properties of materials for 3D printing at high frequencies. Res. Agr. Eng., 69: 28–35.

Abstract: 3D printing is a widely used method. In terms of developing components for electronic devices, it is important to provide good physical properties of the used dielectric. The main parameters are the optional and stable value of the relative permittivity and the minimum dielectric losses of the material. The paper focuses on testing the loss factor and relative permittivity of the following materials: polylactic acid (PLA, in two dye modifications), polyethylene terephthalate glycol (PET-G) and acrylonitrile butadiene styrene (ABS) in the frequency range of 1–100 MHz. It was proven that the values of permittivity of the tested materials were 2.9–4.2 and the loss factor was 0.8–4%. Concerning the relative permittivity, the tendency to show a mild linear drop was observed by increasing the frequency, especially expressed in the PLA materials. With the loss factor, the PLA materials displayed increasing values with an increasing frequency, whereas a declining curve was observed in the PET-G materials. The absolute value of the ABS loss factor varied between 0.9–1.5%. The reasonable influence of added dyes was elucidated upon.

Keywords: ABS; fused deposition modelling (FDM); loss factor; PET-G; PLA; relative permittivity

3D printing is a widespread and rapidly evolving technology that has found its application in multiple industrial areas, such as aerospace, the automotive industry, in medical instruments and devices, spare parts manufacturing, soft robotics or other technology branches (Ning et al. 2015; Stano et al. 2020; Vujović et al. 2021). The other area where the 3D printing is starting to be rapidly applied is agriculture. Common applications in agriculture are the rapid prototyping process of spare parts for repairing agricultural machines, harvesting grippers and for developing capacitive sensors for estimating the soil moisture (Jiménez et al. 2019; Łukaszewski et al. 2021; Kurbah et al. 2022). The use of 3D printing for the manufacturing of capacitive probes for soil moisture measurements is very useful, as this technology enables the low-cost development and production of probes with variable dielectric shapes (Farooqui and Kishk 2018). 3D printing is also used to develop components of electronic tongue (e-tongue) devices which are multisensory systems used in the analysis of complex liquid media based on the impedimetric principle. In the field of precision agriculture, these systems allow one to locally

Supported by the internal research project of the Czech University of Life Sciences Prague, Faculty of Engineering, Czech Republic, Project No: IGA 2019:31200/1312/3112.

https://doi.org/10.17221/10/2022-RAE

monitor the level of plant nutrients available in the soil, with the aim of having a variable-rate fertiliser application. In the case of e-tongue systems, the 3D printing using conductive filaments is being tested as an alternative method of manufacturing the measuring electrodes of the device compared to conventional photolithography. According to (da Silva et al. 2019), electrodes made from 3D printing exhibit good reproducibility results that are comparable to traditionally manufactured electrodes.

In the case of our study, the 3D printing technology was used to develop a device for the automatic measurement of the ice thickness for fish farming, in which the monitoring of ice thickness during the winter months is an important parameter to ensure the oxygen supply to the farmed fish. For this purpose, we developed capacitance probe, which was manufactured using 3D printing.

3D printing provides rapid prototyping, versatility and low production costs (Felício et al. 2016; Dichtl et al. 2017; Veselý et al. 2018a). This technology is expanding mainly due to the open-source project of RepRap (self-replicating rapid prototyper). From 2004, this branch of 3D printing has reasonably developed as the technology is cheap and available for both professionals and home users (Roberson et al. 2013; Irwin et al. 2015).

Fused Deposition Modelling (FDM) is a very frequently used technique for 3D printing. It is a production method called additive manufacturing (AM), which can be defined as a process of layering the above-mentioned materials into the shape of the designed objects (Ning et al. 2015; Veselý et al. 2018b). At present, these technologies are used more and more in the automated production of electronic and electromechanical devices (Espalin et al. 2014). For this reason, the materials must be studied in terms of their dielectric properties. The direct implementation of an electric component into printed subjects is an additional argument for further studies in this field (e.g., electrical conductivity, permittivity, loss factor, etc.) (Palmer et al. 2006; Lopes et al. 2012; Wicker and MacDonald 2012; Billah at al. 2019). 3D printing is also used by number of research laboratories in the production of dielectric components, for instance, antennas (Le Sage 2016; Rashidian et al. 2016; Helena et al. 2021). The other area where it is very useful to use 3D printing technology is the development and manufacturing of capacitance probes. This technology enables one to create dielectrics isolators of various shapes and, in a similar way, this procedure was used in our work to develop the capacitance ice thickness measurement device. The evaluation of the developed sensor capacity was performed by measuring the resonant frequency of the oscillator tuned circuit in which the capacity sensor was connected. These probe parts had to be made of a high-quality insulator that has a constant relative permittivity and a low loss factor value in the frequency range of 3 to 10 MHz, which was the intended operating frequency of the measuring device. For this reason, it was necessary to choose a suitable material with the appropriate dielectric properties.

FDM is the process based on the extrusion and deposition of a multi filament in layers to create a final 3D object, where the layers are joined by a polymerisation reaction between the individual layers (Patterson et al. 2019).

The most common used materials for 3D printing are polylactic acid (PLA), polyethylene terephthalate glycol (PET- G) and acrylonitrile butadiene styrene (ABS) (Veselý et al. 2018a).

Compared to PLA, ABS materials are much more demanding for 3D printing, mainly due to printing at higher temperatures up to 230–250 °C (Birouas and Nilgesz 2017), as the printing materials are subjected to large volume changes (thermal expansion) at this temperature, which results in changes of dielectric properties (Birouas and Nilgesz 2017). Inhomogeneity of this type can modify the dielectric properties of final object. Recently, the permittivity and loss factor of printing materials are known to be in the range of low frequencies (50–100 Hz, and sporadically at 100 kHz) and at ultra-high frequencies (1 GHz and higher). The parameters that are necessary for the development of our equipment (ice thickness indicator) and to operate in the frequency range of 3 to 10 MHz are not published. Dichtl et al. (2017) studied the PLA properties at frequencies of 1 Hz to 3 GHz, but only two measurements (1 and 75 MHz) were made in the high frequencies.

It is important to realise that to replace the missing values by simple extrapolation to the frequencies that are distant from the exactly tested ones is misleading because each relaxation process causes drop in the permittivity and a local increase in the loss factor in the dielectric material related to its time constant. The typical course of this phenomenon is shown on Figure 1 and Figure 2, where the drop of permittivity and increase in the loss factor due to relaxation process with a time constant 10^{-7}s is shown. This influence is the most pronounced

https://doi.org/10.17221/10/2022-RAE

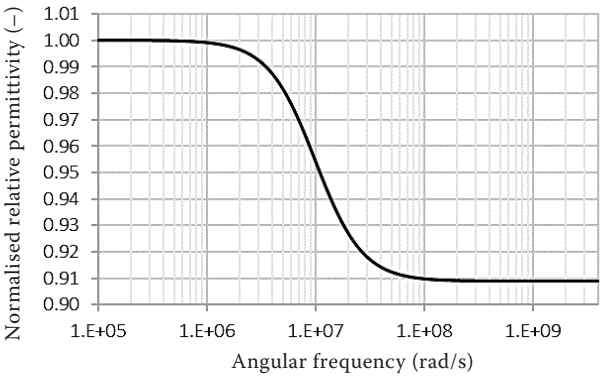

Figure 1. Frequency dependence of the normalised relative permittivity (Havriliak and Havriliak 1997)

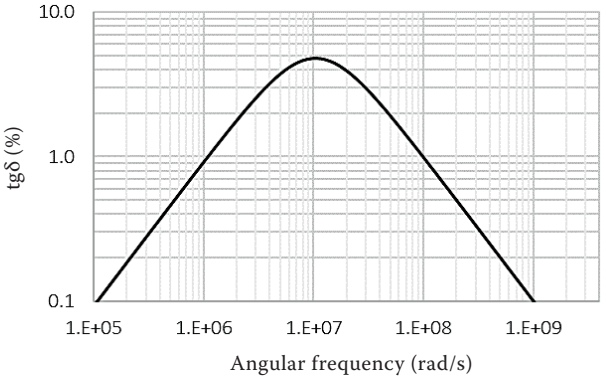

Figure 2. Frequency dependence of the loss factor tgδ (Havriliak and Havriliak 1997)

at the angular frequency corresponding to the inverse value of the time constant (Havriliak and Havriliak 1997). The phenomenon can occur in areas one decade wide above and below this frequency. Polarisation does not occur in more remote areas.

It is not possible to deduce the properties of dielectrics in the field of high frequencies (HF) from the results of the available publications. The values of dielectric properties of the basic materials under the same conditions that have been published in different publications differ by tens of percent (Booth et al. 2017; Novac et al. 2017). The phenomenon is probably caused due to the existence of many relaxation processes in the basic materials and mainly due to the existence of other admixture composites. Therefore, it is necessary to get acquainted with the properties of materials used for 3D printing in more detail. This paper is focused on the comparison of dielectric properties, such as the loss factor and relative permittivity of the applied materials, which have not yet been studied extensively and more precise values have not been possible to obtain from manufacturers of printing materials due to production secrets.

MATERIAL AND METHODS

Tested samples. The tested samples were prepared as a square-shaped plate with a side length of 70 mm and a thickness of 1.6 mm (Figure 3), which were made of PLA, PET-G and ABS. The PLA samples were fabricated in two different colours (silver and metallic green) to compare the effect of the pigment dye on the dielectric properties of the material. The samples of the remaining materials were made in one colour, PET-G in ultramarine blue and ABS in silver.

The samples were printed with a Prusa i3 MK3 3D printer (Prusa Research, Czech Republic) (FDM technology) which is based on the RepRap concept. All the samples were printed at a resolution of 150 μm, with a fill density of 100% and a fill angle of 45°. The tested sample parameters, including the print settings, are summarised in Table 1.

Measuring the dielectric properties. HP 4291A and Agilent 4991A impedance/material analysers (Agilent Technologies, USA)were used for the measurements. As the HP 4291A is more precise in evaluating high impedances, it was especially used for measurements at the lowest frequencies where the impedance of the measuring capacitor is high.

The Agilent 16453A dielectric material test fixture, which is an accessory of both impedance/material analysers, was not used for the measurement, as its use would lead to significant measurement inaccuracies.

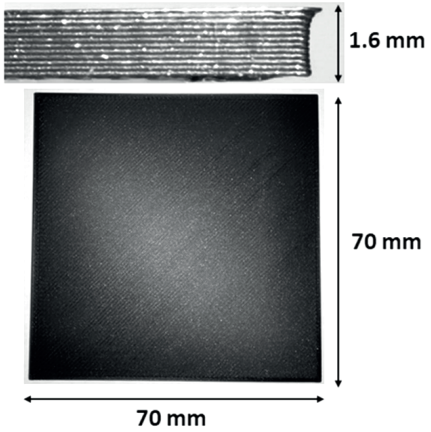

Figure 3. Dimensions of the sample with details of the sample thickness (thickness of 1.6 mm)

https://doi.org/10.17221/10/2022-RAE

Table 1. Sample properties and printing settings.

Sample identification	Material	Colour	Printing temperature (°C)	Printing resolution (µm)	Filament manufacturer	Filament diameter (mm)
PLA-Silver	PLA	silver	210	150	Filament PM	1.75
PLA-Metallic Green		metallic green				
PET-G	PET-G	ultramarine blue	240			
ABS	ABS	silver	255			

PLA – polylactic acid; PET-G – polyethylene terephthalate glycol; ABS – acrylonitrile butadiene styrene

According to the manufacturer (Agilent Technologies 2003), it has a typical inaccuracy in measuring permittivity of approximately 50% for samples with a thickness of a few millimetres and a relative permittivity of the order of units at frequencies below 4 MHz and 15 to 25% in the frequency range 15 to 100 MHz.

Therefore, a measuring fixture of our own design with a three-plate measuring capacitor arrangement with an electrode area of 40 cm^2 was used. It has an approximately two orders of magnitude larger measuring capacity that allows approximately a tenfold reduction in the measurement error in the frequency range up to 100 MHz compared to the Agilent 16453A dielectric material test fixture. The measuring fixture with a sample was connected to the impedance/material analyser via an HP 16093A Binding Post Fixture.

The Agilent 4991A testing device is shown in the Figure 4. It consisted of the above-mentioned the Agilent analyser, an HP 16093A Binding Post Fixture and the measuring fixture of our own design with the analysed sample.

The evaluation was realised in the range of 1–100 MHz. The circuit diagram is shown in Figure 5. The measuring device provides the circuit parameters – total capacitance (C_p) and its quality factor (Q). The relationship between these two parameters is described by Equation (1). The total capacitance consists of the parasitic capacitance of the supply conductors of the electrodes (C_{par}) and the capacitance of the tested sample (C_s). The loss factor (tgδ) is then calculated from the data (Q) according to Equation (2).

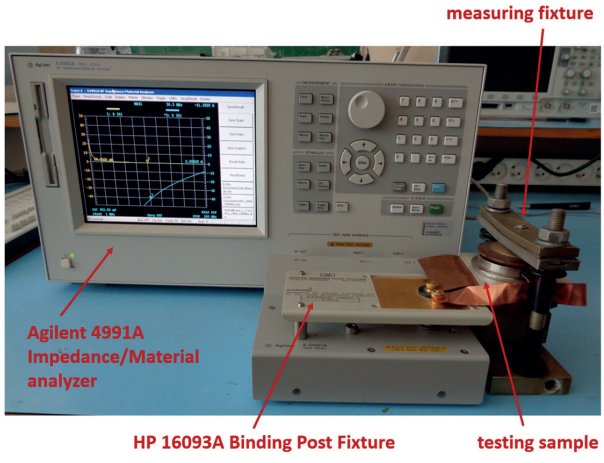

Figure 4. Testing workspace equipped by an Agilent 4991A impedance/material analyser

$$Q = \omega \times C_p \times R \quad (1)$$

where: Q – capacitance quality factor (–); C_p – total capacitance of the measured system (F); R – sample loss resistance (Ω).

$$tg\delta = 100\frac{1}{\omega C_s R} = 100\frac{C_p}{QC_s} \quad (2)$$

where: tgδ – loss factor of the sample (%), C_s – capacitance of the measured sample (F).

The value of the relative permittivity is determined proportionally from the capacitance of examined sample and the capacitance of the Teflon standard. Conversion is preformed using the Equations:

$$C_s = C_p - C_{par} \quad (3)$$

$$C_t = C_p - C_{par} \quad (4)$$

$$\varepsilon_r = \varepsilon_t \frac{C_s t_s}{C_t t_t} \quad (5)$$

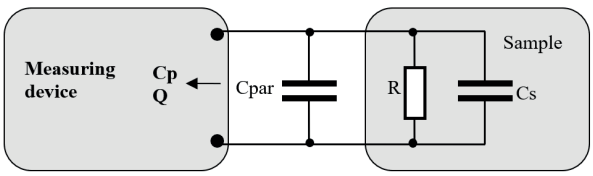

Figure 5. Block diagram of the measuring system

https://doi.org/10.17221/10/2022-RAE

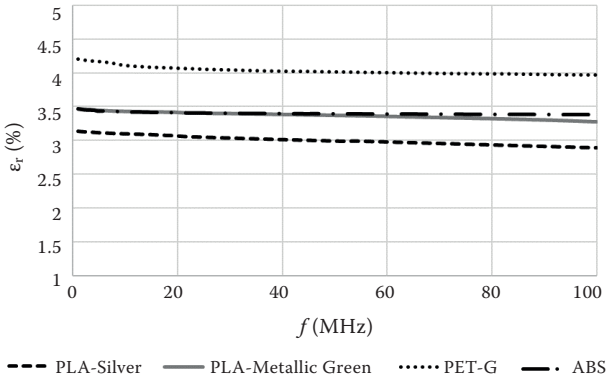

Figure 6. Frequency dependence (f) of the relative permittivity (ε_r) of the selected materials

PLA – polylactic acid; PET-G – polyethylene terephthalate glycol; ABS – acrylonitrile butadiene styrene

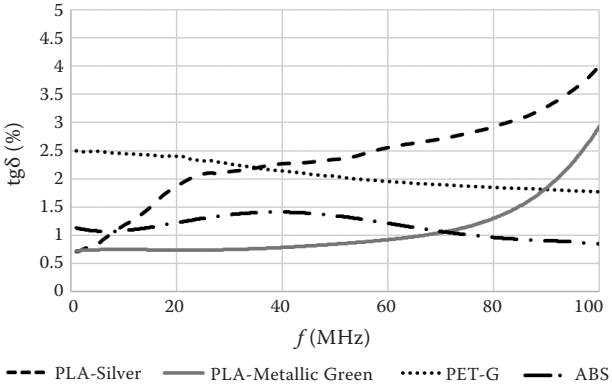

Figure 7. Frequency dependence (f) of the loss factor (tgδ) of the selected materials

PLA – polylactic acid; PET-G – polyethylene terephthalate glycol; ABS – acrylonitrile butadiene styrene

where: C_{par} – parasitic capacitance of the measuring wires (1.78 pF); C_t – capacitance of the Teflon control sample (pF); ε_r – relative permittivity of the measured sample (–); ε_t – relative Teflon permittivity (2.1); t_s – sample thickness (mm); t_t – Teflon standard thickness (1 mm).

Statistical analysis. The raw data for construction of the graphs were processed by the statistical method of a simple moving average (10 was the base of the period). This data processing was performed for a better graphical data presentation. Similarly, the raw data were used for the evaluation of the relative permittivity and loss factor, the measuring interval was divided into three intervals (1–4.9, 5–49.9 and 50–100 MHz). The frequency range was divided into these three intervals for the more precise description of the measured material parameters. The average and standard deviation of the relative permittivity and loss factor were calculated for each interval.

RESULTS

The results are presented in Figures 6 and 7. The graph in Figure 6 expresses the frequency relations of the relative permittivity of all the tested materials (PLA-Silver, PLA-Metallic Green, PET-G and ABS). It can be seen that the permittivity values were in interval 2.9–4.2. The curves of the PLA-Metallic Green and ABS are practically identical. The PLA-Silver and PET-G differed in the absolute values – the average absolute value in PLA-Silver was 3.12 (1–4.9 MHz; Table 2), whereas a relative permittivity of 4.21 was found for PET-G at the same frequency. Through measurement in the interval 1–100 MHz, the permittivity value insignificantly changed having a practically linear shape in all the curves and a slightly decreasing tendency was observed in the higher frequency region. It was ascertained that both the PLA materials (different colours) differed

Table 2. Statistical evaluation of the measured data of the relative permittivity (ε_r) and the loss factor (tgδ)

Sample identification	1–4.9 MHz				5–49.9 MHz				50–100 MHz			
	ε_r		tgδ		ε_r		tgδ		ε_r		tgδ	
	aver.	error	aver.	error	aver.	error	aver.	error	aver.	error	aver.	error
	(–)		(%)		(–)		(%)		(–)		(%)	
PLA-Silver	3.12	0.31	0.85	0.13	3.04	0.06	1.99	0.2	2.94	0.04	3	0.3
PLA-Metallic Green	3.45	0.35	0.74	0.11	3.4	0.07	0.76	0.08	3.32	0.05	1.49	0.15
PET-G	4.21	0.67–0.84	2.36	0.35	4.06	0.2	2.29	0.23	3.99	0.06–0.08	1.87	0.19
ABS	3.45	0.55–0.69	1	0.15	3.41	0.17	1.33	0.13	3.38	0.05–0.07	1	0.1

aver. – average value of the relative permittivity and loss factor; error –standard deviation of the relative permittivity and loss factor; PLA – polylactic acid; PET-G – polyethylene terephthalate glycol; ABS – acrylonitrile butadiene styrene

https://doi.org/10.17221/10/2022-RAE

in the absolute value of the permittivity, but the slopes of the curves were the same.

The frequency dependence of the loss factor of the tested materials is summarised in Figure 7. It can be seen the values of the loss factor were 0.8–4% in tested interval. The PLA-Silver and Metallic Green curves shoved a similar general shape with a slightly increasing absolute value of the loss factor in the region of higher frequencies. The maximal increase was in the range 70–100 MHz. However, these two curves substantially differed by their course in the interval 1–20 MHz. Here, the relative significant and linear increase in the loss factor was found in the PLA-Silver compared to the PLA-Metallic green. Both curves have a similar and parallel shape from a frequency of 20 MHz. The frequency dependence of the loss factor of the remaining two materials differed, especially in the absolute values. In the ABS material, this parameter slightly varied in the interval 1–1.5% whereas in the PET-G material, it had a rather descending tendency (2.5 to 1.8%).

The particular values of the relative permittivity and loss factor in the assessed frequency intervals are summarised in Table 2. The examined range was divided into three intervals: 1–4.9, 5–49.9 and 50–100 MHz. The directly measured data were subsequently processed statistically (average and standard deviation) and, in this manner, the tabulated data are provided for potential practical use. Of course, the data fully correspond to the data in the graphs (Figure 6 and 7).

The values of the relative permittivity of the PLA-Silver and PLA-Metallic Green show the difference in the entire measured range. In all three frequencies ranges (1–4.9, 5–49.9 and 50–100 MHz), the difference was set to 0.33, 0.36, and 0.38.

The difference between the loss factors of both PLA materials reached 0.11%, 1.23% and 1.51% in all three above-mentioned intervals.

DISCUSSION

The results show that values of the relative permittivity varied between 2.9–4.2 and the values of the loss factor were in the range 0.8–4.0%. These results showed the additional important fact that, in terms of the relative permittivity, the PLA materials exhibit a linear relationship within the entire examined frequency range. Moreover, a very mild decrease in the permittivity was observed with the increasing frequency. The frequency dependence of the relative permittivity of the PET-G and ABS materials manifested itself as a slightly decreasing one with the increasing frequency.

As regards to the loss factor, the most suitable one for electrical applications appears to be PLA-Metallic Green, whose factor reached its lowest values up to 70 MHz and showed a minimal frequency dependence. The results are in concordance with those of Dichtl et al. (2017). At higher frequencies, however, it exhibited an exponential increase which reduces its use up to this limit. Another material that appears to be suitable in terms of the loss factor is PET-G, which reached, in general, the smallest frequency dependence within the entire measured range, but, at the same time, it is disadvantaged by significantly higher values at lower frequencies (up to 30 MHz). ABS can be suitable as well due to the low values of the loss factor (0.9–1.5%) over the whole measuring range and the small curve changes in the middle part can be considered insignificant. The PLA-Silver material appears to be less suitable in this respect due to the higher frequency dependence within the entire measured range. The difference between these two PLA materials is probably caused by using different dyes. A similar phenomenon was observed with the PLA materials by Veselý et al. (2018a).

It should also be noted that additional differences were observed between the individual PLA materials concerning the loss factor. This phenomenon can be explained by the different composition of the dyes in both materials, which was also described by Veselý et al. (2018a).

CONCLUSION

Today, 3D printing is a widespread and rapidly developing technology due to the possibility of rapid prototyping and low production costs. In the field of agriculture, this technology is now mainly used in the development of spare parts for agricultural machinery, harvesting grippers, as well as in capacitance and chemical sensors. In the field of sensor development, this technology represents an alternative to conventionally used manufacturing technologies and, for this reason, it seems very useful to study the dielectric properties of materials used for 3D printing in more detail, which have not been studied in the tested range (1–100 MHz).

The paper is focused on the comparison of dielectric properties, such as the relative permittivity and the loss factor of PLA, PET-G and ABS materials.

https://doi.org/10.17221/10/2022-RAE

The parameters were measured in the frequency range of 1–100 MHz.

The conclusions of this research:

(1) The values of the relative permittivity varied between 2.9–4.2 and the values of the loss factor were in the range 0.8–4.0%.

(2) In terms of the relative permittivity, all the materials exhibit a linear relationship within the entire examined frequency range. Moreover, a very mild decrease in the permittivity was observed with an increasing frequency. The maximal difference was found between PLA-Silver and PET-G (1.09 at frequency 1–4.9 MHz). As regards to the loss factor, the most suitable materials for electrical applications appears to be PLA-Metallic Green whose factor reached its lowest values up to 70 MHz and showed a minimal frequency dependence.

(3) In terms of the loss factor, the PET-G materials seemed the best which reached, in general, the smallest frequency dependence, but it is disadvantaged by significantly higher values at lower frequencies (up to 30 MHz).

(4) ABS can be suitable as well due to the low values of the loss factor (0.9–1.5%). The PLA-Silver material appears to be less suitable due to the higher frequency dependence. The difference between the two PLA materials can be caused by using different dyes.

(5) Additional differences were observed between the individual PLA materials considering the loss factor, which can be caused by the different composition of the dyes in both materials as it is not possible to automatically expect the same dielectric properties, when applying the same type of materials, but with different colour pigmentations.

The obtained results of this study are going to be used for the development of capacitance probes for the non-destructive measurement of ice thickness.

Acknowledgement: The authors thank the Czech Technical University in Prague, Faculty of Electrical Engineering for enabling the measurement of the quality factor and the total capacity of the tested samples.

REFERENCES

Agilent Technologies (2003): Agilent E4991A RF Impedance/Material Analyzer Data Sheet. Agilent Technologies, Inc., USA: 6–7.

Billah K.M.M., Coronel J.L., Halbig M.C., Wicker R.B., Espalin D. (2019): Electrical and thermal characterization of 3D printed thermoplastic parts with embedded wires for high current-carrying applications. IEEE Access, 7: 18799–18810.

Birouas F.I., Nilgesz A. (2017): Prototyping robotic medical rehabilitation devices. Nonconventional Technologies Review, 21: 51–56.

Booth J.C., Whitley M., Rudd C., Kranz M. (2017): Material database for additive manufacturing techniques. Defense Technical Information Center, 2017: 1–37.

da Silva T.A., Braunger M.L., Coutinho M.A.N., do Amaral L.R., Rodrigues V., Riul A. (2019): 3D-printed graphene electrodes applied in an impedimetric electronic tongue for soil analysis. Chemosensors, 7: 1–11.

Dichtl C., Sippel P., Krohns S. (2017): Dielectric properties of 3D printed polylactic acid. Advances in Material Science and Engineering, 2017: 6913835.

Espalin D., Muse D.W., Macdonald E., Wicker R.B. (2014): 3D printing multifunctionality: Structures with electronics large format additive manufacturing of fiber reinforced thermoplastic composite view project IOT for casting view project 3D printing multifunctionality: Structures with electronics. International Journal of Advanced Manufacturing Technology, 72: 963–978.

Farooqui F.M., Kishk A.A. (2018): Low-cost 3D-printed wireless soil moisture sensor. In: 2018 IEEE Sensors, New Delhi, Oct 28–31, 2018: 1–3.

Felício J.M., Fernandes C.A., Costa J.R. (2016): Complex permittivity and anisotropy measurement of 3D-printed PLA at microwaves and millimeter-waves. In: Proc. Int. Conf. Applied Electromagnetics and Communications – ICECOM, Dubrovnik, Sept 19–21, 2016: 1–6.

Havriliak S., Havriliak S.J. (1997): Dielectric and Mechanical Relaxation in Materials, Analysis, Interpretation, and Application to Polymers. Munich, Carl Hanser Verlag: 378–400.

Helena D., Ramos A., Varum T., Matos J.N. (2021): The use of 3D printing technology for manufacturing metal antennas in the 5G/IoT context. Sensors, 21: 3321.

Irwin J.L., Oppliger D., Pearce J.M., Anzalone G. (2015): Evaluation of RepRap 3D printer workshops in K-12 STEM. In: Proc. 2015 ASEE Annual Conference and Exposition, Seattle, June 14–17, 2015: 1–18.

Jiménez A.D.L.Á.C., Almeida C.D.G.C.D, Santos Júnior J.A., Morais J.E.F.D., Almeida B.G.D., Andrade F.H.N.D. (2019): Accuracy of capacitive sensors for estimating soil moisture in northeastern Brazil. Soil and Tillage Research, 195: 104413.

Kurbah F., Marwein S., Marngar T., Sarkar B.K. (2022): Design and development of the pineapple harvesting robotic gripper. Smart Innovation, Systems and Technologies, 229: 437–454.

https://doi.org/10.17221/10/2022-RAE

Le Sage G.P. (2016): 3D printed waveguide slot array antennas. IEEE Access, 4: 1258–1265.

Lopes A.J., MacDonald E., Wicker R.B. (2012): Integrating stereolithography and direct print technologies for 3D structural electronics fabrication. Rapid Prototyping Journal, 18: 129–143.

Łukaszewski K., Buchwald T., Wichniarek R. (2021): The FDM technique in processes of prototyping spare parts for servicing and repairing agricultural machines: A general outline. International Journal of Applied Mechanics and Engineering, 26: 145–155.

Ning F., Cong W., Wei J., Wang S., Zhang M. (2015): Additive manufacturing of CFRP composites using fused deposition modeling: Effects of carbon fiber content and length. In: Proc. ASME 2015 Int. Manufacturing Science and Engineering Conf. MSEC2015, Charlotte, June 8–12, 2015: 1–7.

Novac O.C., Maries G.R.E., Chira D., Novac M. (2017): Study concerning the influence of the grinding percentage on some electrical properties of PA 6.6, POM and ABS by methods for determining relative permittivity and the dielectric dissipation factor. Materiale Plastice, 54: 453–460.

Palmer J.A., Jokiel B., Nordquist, C.D., Kast B.A., Atwood C.J., Grant E., Livingston F.J., Medina F., Wicker R.B. (2006): Mesoscale RF relay enabled by integrated rapid manufacturing. Rapid Prototyping Journal, 12: 148–155.

Patterson A.E., Pereira T.R., Allison J.T., Messimer S.L. (2019): IZOD impact properties of full-density fused deposition modeling polymer materials with respect to raster angle and print orientation. Proceedings of the Institution of Mechanical Engineers, Part C: Journal of Mechanical Engineering Science, 2019: 146523727.

Rashidian A., Shafai L., Sobocinski M., Perantie J., Juuti J., Jantunen H. (2016): Printable planar dielectric antennas. IEEE Transactions on Antennas and Propagation, 64: 403–413.

Roberson D.A., Espalin D., Wicker R.B. (2013): 3D printer selection: A decision-making evaluation and ranking model. Virtual and Physical Prototyping, 8: 201–212.

Stano G., Arleo L., Percoco G. (2020): Additive manufacturing for soft robotics: Design and fabrication of airtight, monolithic bending pneunets with embedded air connectors. Micromachines, 11: 485.

Veselý P., Horynová E., Tichý T., Šefl O. (2018a): Study of electrical properties of 3D printed objects. In: Husník L.: Proc. Int. Student Scientific Conf. Poster, Prague, May 10**,** 2018: 1–5.

Veselý P., Tichý T., Šefl O. Hornyová E. (2018b): Evaluation of dielectric properties of 3D printed objects based on printing resolution. IOP Conference Series: Materials Science and Engineering, 461: 1–6.

Vujović I., Šoda J., Kuzmanić I., Petković M. (2021): Parameters evaluation in 3D spare parts printing. Electronics, 10: 365.

Wicker R.B., MacDonald E.W. (2012): Multi-material, multi-technology stereolithography: This feature article covers a decade of research into tackling one of the major challenges of the stereolithography technique, which is including multiple materials in one construct. Virtual and Physical Prototyping, 7: 181–194.

Received: February 5, 2022
Accepted: June 13, 2022
Published online: December 20, 2022